Instantaneous Doppler Global Velocimetry Measurements of a Rotor Wake: Lessons Learned

James F. Meyers
Gary A. Fleming
NASA Langley Research Center
Hampton, Virginia 23681 USA

and

Susan Althoff Gorton
John D. Berry
Aeroflightdynamics Directorate (AVRDEC)
U. S. Army Aviation and Missile Command
Langley Research Center
Hampton, Virginia 23681 USA

9th International Symposium on Applications of Laser Techniques to Fluid Mechanics
Lisbon, Portugal
July 13-16, 1998

Instantaneous Doppler Global VelocimetryMeasurements of a Rotor Wake: Lessons Learned

James F. Meyers
Gary A. Fleming
National Aeronautics and Space Administration
Langley Research Center
Hampton, Virginia 23681 USA

and

Susan Althoff Gorton
John D. Berry
Aeroflightdynamics Directorate (AVRDEC)
U. S. Army Aviation and Missile Command
Langley Research Center
Hampton, Virginia 23681 USA

Abstract

A combined Doppler Global Velocimetry (DGV) and Projection Moiré Interferometry (PMI) investigation of a helicopter rotor wake flow field and rotor blade deformation is presented. The three-component DGV system uses a single-frequency, frequency-doubled Nd:YAG laser to obtain instantaneous velocity measurements in the flow. The PMI system uses a pulsed laser-diode bar to obtain blade bending and twist measurements at the same instant that DGV measured the flow. The application of pulse lasers to DGV and PMI in large-scale wind tunnel applications represents a major step forward in the development of these technologies. As such, a great deal was learned about the difficulties of using these instruments to obtain instantaneous measurements in large facilities. Laser speckle and other image noise in the DGV data images were found to be traceable to the Nd:YAG laser. Although image processing techniques were used to virtually eliminate laser speckle noise, the source of low-frequency image noise is still under investigation. The PMI results agreed well with theoretical predictions of blade bending and twist.

Introduction

The precise prediction of the helicopter main rotor wake has been cited as the driving factor for accurately predicting rotor loads, vibration, performance, and noise. It is widely accepted throughout the rotorcraft industry that correctly modeling the wake geometry and the tip vortex formation, size, strength, and position are essential to a numerical solution of the wake problem. Although there have been many efforts to characterize the rotor wake using various methods of flow visualization, these qualitative efforts are insufficient to validate and improve the numerical models of the rotor wake. Detailed, quantitative flowfield information is required.

The acquisition of the requisite flowfield measurements has been impeded by the harsh environment in which a rotor blade operates. Since the blades rotate, the flow environment is constantly changing, and each blade is affected by the wake structure shed from the preceding blades. Thus, investigations of this unsteady, vortex-dominated flow require measurement techniques that are: 1) nonintrusive, 2) instantaneous, 3) simultaneous three-component, and 4) correlated with rotor azimuth. Although fringe-type laser velocimetry satisfies the measurement requirements, the excessive acquisition time needed to obtain statistically-significant, azimuth-dependent results makes the technique impractical for surveying large areas within the rotor flowfield. Particle Image Velocimetry is limited to two dimensional measurements over relatively small measurement planes in large wind tunnel applications.

For the past several years, the NASA Langley Research Center has been developing Doppler Global Velocimetry (DGV) for use in large wind tunnels. DGV is a planar measurement technique capable of obtaining three-component flow field velocity data. Previous applications of DGV used a continuous-wave (CW) Argon-ion laser and produced flow velocity measurements that were temporally integrated over the 16.7 ms CCD camera exposure. Demonstrations of the instrument operating in this manner included the detailed measurement of wing tip vortices at focal distances of 18 m (Meyers (1996)). While these integration times were satisfactory for the measurement of stationary flows, they were unacceptable for the measurement of the unsteady flows found in rotorcraft applications. In anticipation of this limitation, the Northrop Research and Technology Center was contracted by the NASA Langley Research Center in 1990 (Komine *et al* (1994)) to conduct laboratory investigations to determine if a single-frequency, frequency-doubled Nd:YAG laser could be used in DGV applications to obtain instantaneous velocity measurements. This successful research program culminated with the first

instantaneous DGV measurements, as demonstrated by one-component velocity measurements in a 10-x 10-cm free jet.

The subject of this investigation was the rotor wake developed by an isolated rotor system consisting of a Mach-scaled, four bladed rotor with a rotor disk diameter of 1.7 m. A scaled, generic helicopter fuselage shell, independent of the rotor drive system and hub, could be raised from the tunnel floor to investigate its effect on the flow and nonlinear interactions with the rotor wake. The primary objective of the current investigation was to integrate the three-component DGV technology developed by NASA with the experience derived from the Northrop effort to create an instrumentation system capable of measuring the unsteady rotor wake flow field. Complete diagnostics of the rotor wake must include blade deformation and position data since the rotor wake geometry is largely affected by these parameters. A second objective was to use the newly advanced capabilities of a laser diode-based Projection Moiré Interferometer to obtain blade position, bending, and twist data at the same instant as the velocity field was measured with the DGV system.

Experimental Facilities

The experiment was performed in the Langley 14-by 22-Foot Subsonic Tunnel shown in Figure 1 (Gentry *et al* (1990)). This atmospheric, closed-circuit low-speed wind tunnel can be operated with a closed test section, or by raising the walls and ceiling, in an open test section mode. For this study, the tunnel was operated as a modified open test section with the walls raised for maximum optical access to the rotor wake, and the ceiling lowered to serve as a mounting platform for the isolated rotor drive system. The wind tunnel is equipped with propylene glycol vaporization/ condensation smoke generators that were mounted on a traversing mechanism located in the tunnel settling chamber.

The isolated rotor test system (IRTS) is a general-purpose rotor testing system. The fully articulated hub holds a Mach-scaled, four-bladed, 1.7-meter diameter rotor. The rotor blades have a rectangular planform and an NACA 0012 airfoil section with a chord of 6.6 cm and a linear twist of -8 degrees, nose down. Note that the rotor blades are very stiff torsionally when compared with a full-scale rotor system. A digital 1024 pulse per revolution encoder was attached to the rotor shaft to monitor rotor speed and provide an azimuthal record for conditionally sampling the instrumentation systems. A helicopter fuselage model was mounted on a vertical strut below the rotor. The strut could be raised and lowered to locate the fuselage in proper position under the rotor, Figure 2, or fully lowered to be out of the

influence of the rotor wake, Figure 3. A conventional, 3-D Laser Velocimeter was also used during the test to acquire a limited number of velocity measurements in the rotor wake.

Doppler Global Velocimeter

The Doppler Global Velocimeter is an Iodine vapor cell based, three-component system utilizing a pulsed, single-frequency, frequency-doubled Nd:YAG laser to obtain instantaneous (10 ns) measurements. The description of DGV technology is given by Komine (1990) and Meyers (1995). The system consists of the Nd:YAG laser, light sheet forming optics, laser frequency monitoring system, and three receiver optical systems. The output laser beam was directed to the light sheet forming optics located on the wind tunnel test section floor, Figures 2 and 3. The receiver optical systems and the laser frequency monitoring system consisted of a linear polarizer, beamsplitter, an encased and insulated Iodine vapor cell, mirror, and two electronically shuttered CCD video cameras, Figure 4. Each system was enclosed to protect the optics from the wind tunnel environment and flow buffeting.

All three receiver optical systems were placed on the advancing side of the rotor to have an unobstructed view of the laser light sheet when the fuselage was in place, Figure 5. Their placement yielded an angle between the vector measured by component A and the vector measured by component B of 52 degrees, 47 degrees between the vectors measured by components A and C, and 41 degrees between the vectors measured by components B and C. These separation angles were sufficient to minimize trigonometric errors when translating the measurements to the streamwise, vertical, and crossflow velocity components. The common field of view was an area 1.02-by 1.14 meters.

The data acquisition system consists of a network of five PC compatible computers with one computer dedicated to each measurement component, the fourth obtaining data from the laser frequency monitor, and the fifth serving as the operator terminal and system controller. Each component computer contains two 10-bit frame grabbers to acquire single-field (512x256 pixels) images from the signal and reference cameras, respectively. The industry standard RS-170 cameras were electronically shuttered (0.1 ms) in synchronization with the Nd:YAG laser. While the cameras and data acquisition system were set to free run, images were only acquired when the rotor shaft encoder aligned with one of the selected azimuth angles: 0- to 90-degrees, in 10 $\pm$0.7 degrees ($\pm$2 encoder steps) increments.

Projection Moiré Interferometer

Conventional projection moiré interferometry begins with the projection of a grid of equispaced, parallel lines onto the surface of a test object. With the object in the reference condition, a CCD video camera is used to acquire an image of the object illuminated by the lines. When the object is deformed, the grid line spatial arrangement changes. A second image is then acquired. Subtracting the reference image from the data image yields a pattern of moiré fringes tracing the contours of constant deformation amplitude. The measured deformation direction is along the bisector of the projection and viewing vector directions. The deformation amplitude between adjacent moiré fringes is proportional to the projected grid line spacing and the angle between the projection and viewing vectors.

The Projection Moiré Interferometry (PMI) system used in this study was a single-component, laser diode based system capable of obtaining instantaneous (0.1 ms) measurements. This system is described in detail by Fleming and Gorton (1998). The system consists of a pulsed 15 W laser diode bar (10 discrete emitters) operating at 800 nm, a Ronchi ruling, projecting optics, and an electronically shuttered CCD video camera. The laser diode bar was chosen as the light source because of its small size, high output power, single pulse operation, and infrared wavelength. The laser light passes through the Ronchi ruling (a diffracting grading with a square wave cross section) to a lens system that projected the resulting lines onto the underside of the rotor blades, Figure 6. The PMI optical system was placed below the test section floor to view a 1.2-x 1.2-meter area in the rotor disk plane covering 50 degrees of rotor azimuth, Figure 5. The data acquisition system, a one-camera version of the DGV component acquisition system, and the laser diode bar were triggered by the DGV synchronization signal. Thus the DGV and PMI systems acquired data at the same instant with the same measurement window.

The standard PMI reference image could not be obtained since the rotor blades continuously moved through the viewing area. An aluminum honeycomb plate was placed in the rotor disk plane at the rotor hub height to obtain a reference image. Subtraction of this image from the data images produced moiré fringe patterns representing height changes of the rotor blade above this reference plane. Additional processing, described by Fleming and Gorton (1998), yielded the location, bending, and twist of the imaged rotor blade at the instant of the DGV velocity measurement.

Calibration Procedures

As with most optical instrumentation systems, DGV and PMI required daily alignment and system calibration. Their use of video cameras as the measurement sensors eased alignment procedures, but increased the number of calibration techniques needed. The systems were aligned using a simple target of equispaced dots shown in Figure 7. Each DGV component receiver optical system was aligned using a custom electronics system to normalize the signal camera image by the reference camera image in real time. Adjusting the signal camera position and viewing angle to the proper alignment would extinguish the dots from the normalized image. Aligning the PMI was even simpler: align the viewing camera to keep the dot pattern as square as possible, then focus the projected grid lines to fill the viewing area and obtain optimal contrast.

Daily calibration of the instruments more extensive system alignment was necessary. Both techniques required optical calibrations to remove optical and perspective distortions from the acquired data images. Spatial distortions were determined using the alignment target, Figure 7, to establish a centroid map for each camera. The maps, which embodied the observed optical and perspective distortions, were used to compute the piecewise bilinear warping coefficients necessary to remove the distortions from the data images (Meyers (1992) and Meyers (1995)). Corrected DGV signal images could then be normalized by their respective corrected reference images to yield the component velocity data images. In addition, the warping procedures were sufficiently accurate to allow the determination of the orthogonal U, V, and W velocity components from the three measured components. Likewise, similar procedures were used to remove spatial distortions from the PMI data images.

Since DGV measurements are based on the ratio of image amplitudes, additional calibrations were required that were not necessary for the spatially-based measurements of the PMI. The amplitude response of each DGV receiver system was flattened by determining the sensitivity of each camera pixel, and measuring any spatially dependent transmission losses through the optics. This process generated a pixel sensitivity correction image for each camera in the DGV system, and an optical transmission correction image for each receiver. When multiplying data images by their respective pixel sensitivity correction image, the overall camera response would be held constant. Likewise, by multiplying the normalized signal images by their respective optical transmission correction image, differences in the transmission of light through the signal and reference optical paths were removed (Meyers (1995)).

The final calibration for DGV determined the Iodine cell transfer function. The Nd:YAG laser output beam was redirected and split into three beams that were then directed to points on the tunnel structure, each within the field of view of their respective receiver optical system. The sampling of the output beam by the laser frequency monitor was also maintained. Tuning the laser frequency through the Iodine absorption line produced the simultaneous calibration of the four cells. This procedure could be performed at any time, even during tunnel operation.

The PMI reference plane was established by replacing the dot target with an aluminum honeycomb plate painted flat white. The laser bar generated the grid of projected lines on the plate. A comparison of the camera image of the projected lines with the images of the dot target yielded the grid line spacing, and thus the sensitivity factor for the moiré fringes (Fleming and Gorton (1998)).

The Test

The Rotor Wake / Configuration Aerodynamics Test was conducted to investigate the three-component velocity flow field within the rotor wake with and without a fuselage placed below the rotor. The measurement of the trajectory and velocity of the rotor tip vortices as they moved downstream was of primary interest. Several instrumentation issues were in question since this was the first attempt at using global instrumentation to quantify the rotor wake. These included the integration of a pulsed, Nd:YAG laser into the DGV system, the ability of PMI to accurately measure instantaneous blade position, bending, and twist, and the logistics behind the simultaneous operation of the DGV and PMI systems with synchronized lasers (2), video cameras (9), and data acquisition systems (6 computers).

Velocity measurements of the rotor wake were desired at the 30-, 80-, 97-, 99-, 101-, and 103-percent span locations. Planar measurements at these spanwise locations would provide enough information to accurately determine the blade tip vortex structure and trajectory in the near rotor wake. The DGV laser light sheet was oriented vertically and directed upstream, Figure 2. An automated beam steering mechanism was devised to position the light sheet within the 97- to 103-percent span locations so that light sheet alignment changes could be made while the tunnel was operating. The 30- and 80-percent locations required realignment of the DGV optics.

Each day of testing began with the alignment of the DGV and PMI optical systems, followed by the spatial calibration of both systems at

the desired span position. A rotor blade was removed during this process to allow unobstructed optical access to the measurement plane. The laser light sheet was then aligned to the span position. Once aligned, the laser beam was redirected to the tunnel structure to conduct the Iodine vapor cell calibrations. The rotor blade was then replaced and the tunnel test section sealed. The rotor was spun to 2,000 rpm and the laser beam redirected to form the light sheet. Note that the rotor was always spinning when the pulsed light sheet was crossing the blades; this technique protected the composite rotor blades from damage by the high-power light sheet. The tunnel speed was then set to 9.1 m/s and the smoke plume positioned to pass through the light sheet at the rotor wake.

Data acquisition began when the rotor system, wind tunnel velocity, and smoke plume position were stable. A portion of the Nd:YAG laser beam was sampled by a fast photodiode whose output was monitored with a high-speed digital oscilloscope. The shape of the photodiode amplitude vs. time trace was visually inspected to determine that the laser operated in single-frequency mode. If the photodiode output signal had a Gaussian amplitude profile, the laser was operating at a single frequency. A series of 100 conditionally sampled DGV and PMI image sets was acquired when single frequency operation was obtained. The laser beam was redirected to the tunnel walls and a sample of ten images was acquired. This provided a measurement of the Iodine vapor calibration stability. The light sheet was reformed and a second acquisition of 100 image sets obtained. Another calibration check was made followed by the acquisition of the third and final data set. The 300 image sets would yield approximately 30 image sets at each of the selected azimuth angles. This process was repeated at tunnel speeds of 27.7 m/s and 42.0 m/s with the fuselage in both high and low positions (Figures 2 and 3).

Effects of Using the Nd:YAG Laser in DGV

Changing the DGV laser source from an Argon-ion laser to a pulsed, single-frequency, frequency-doubled Nd:YAG laser provided the capability to obtain conditionally-sampled rotor azimuth-dependent data. It also simplified Iodine vapor cell calibrations since the optical frequency was continuously tunable. Unfortunately, the change in laser also affected both image quality and frequency stability. Laser speckle was a far greater problem with the Nd:YAG laser than the Argon-ion laser. Although increased speckle might be expected from the narrower linewidth Argon-ion laser (10 MHz vs. 80 MHz for the Nd:YAG), the reverse was found. The level of laser speckle noise expected from the Argon-ion laser was reduced by temporal averaging

the collected particle-scattered light during the 16.7 ms CCD camera integration time.

Classically laser speckle has been removed using low pass filtering techniques. These techniques include temporal averaging, spatial averaging, low frequency camera Modulation Transfer Functions (MTF) (Smith (1998)), data binning (McKenzie (1997)), and image convolution with a filtering kernel (Meyers (1995)). Temporal averaging of conditionally sampled instantaneous data requires an instrument satiability greater than that achieved in the present study. The other techniques have varying potential for removing laser speckle noise. They all low-pass filter the image data. Complete removal of laser speckle noise would require such a low filter bandwidth that the characteristics of flow structures would be masked. Since the data processing software developed for the Argon-ion based system used the image convolution technique, a new method was developed that would remove laser speckle noise without modifying the flow structure data such as for rotor vortices.

A nonlinear filtering technique developed to remove impulse noise without affecting the underlying image integrity is the median filter (Astola and Kuosmanen (1997)). Basically, the technique sorts pixel amplitudes within the processing kernel, e.g., 5x5 pixels, then selects the median amplitude as the filtered result. A median filter removes impulsive noise while the kernel based low pass filter passes an impulse, albeit wider with a lower amplitude. The effectiveness of this filter can be seen by comparing an original reference camera image with the image after filtering, Figure 8. Using this filtering method, laser speckle noise was virtually eliminated from the data images, revealing the rotor wake structures. It also revealed a low spatial-frequency modulation in the normalized signal image not found in the Argon-ion laser based system.

Laser frequency stability greatly deteriorated during the wind tunnel investigation though it was not identified as a potential concern in the laboratory. This can be illustrated by comparing a series of ratio measurements obtained by the laser frequency monitoring system during the rotor wake investigation with a similar series obtained during a subsequent investigation in the Langley Unitary Plan Wind Tunnel, Figure 9. A comparison of the two samples clearly shows a far more stable output frequency from the Nd:YAG laser during the UPWT investigation than the rotor wake test. The difference was traced to the sensitivity of the laser to vibration. The area adjacent to the UPWT test section was equivalent to a laboratory environment. However, the area adjacent to the open test section in the 14-by 22-Foot Subsonic Tunnel proved to be a very hostile. Floor vibration and wind tunnel

shear layer buffeting caused the laser to lose frequency stability. Also, temperature variations, up to 30° C, during tunnel operation affected the Iodine vapor cell temperature stability, thus modifying its absorption characteristics.

Iodine Vapor Cell Stability

The inability of the Iodine vapor cell heating system to compensate for large changes in environmental temperature was discovered during a previous DGV entry in the 14-by 22-Foot Subsonic Tunnel. In preparation for the current investigation, the cells were insulated and encased with a controlled heat sink on the stem to maintain a small, but constant positive heat transfer. Also the cell in the laser frequency monitor was modified to have a limited vapor pressure by reducing the amount of Iodine placed in the cell. In addition, calibrations were conducted before the tunnel run, once during the run between changes in tunnel velocity, and after the tunnel run, along with laser frequency measurements made between the acquisition of data sets. An overlay of these three Iodine cell calibrations for component C from a typical tunnel run is shown in Figure 10. The mismatch in calibration was a result of temperature variations in the cell from 47.4° C, to 48.0° C, to 53.0° C respectively. Since the environmental effects were not eliminated by insulating and encasing the cells, bias errors were present in the velocity measurements. Although the limited-vapor cell temperature also changed, 50.2° C, to 49.8° C, to 52.4° C with the corresponding calibrations shown in Figure 11, the affects on cell calibration were reduced.

Smoke System Seeding

The seeding system for the DGV measurements used a superheated propylene glycol and water mixture. The smoke was injected using the standard flow visualization smoke generator for the tunnel and three additional portable smoke generators all located on a positioning system in the settling chamber of the tunnel. The smoke generators were mounted on an array as shown in Figure 12 which was upstream of the flow straightening honeycomb and four anti-turbulence screens, 26 m upstream from the test section. The smoke output for DGV in this wide field of view application was marginal. Although each of the generators was producing the maximum volume of smoke, the smoke dispersion and distribution in the test section was unsatisfactory to seed the large planar viewing area. In addition, the heated smoke contained its own convective flow patterns at the lowest tunnel speeds.

It was also difficult to locate the smoke plume in the vortex region since the laser could not be synchronized with rotor azimuth.

Rotor Wake Measurements

The objective of the rotor wake measurements was to obtain measurements of the rotor tip vortex trajectory and velocity for several flight conditions, with and without the presence of a fuselage beneath the rotor. The test conditions were chosen to match the conditions for which flow visualization data were reported by Ghee *et al* (1996) as well as to match the conditions for which rotor inflow data were obtained by Elliott *et al* (1988).

Although the bias error limits the usefulness of the DGV data, patterns appear to correlate to the expected behavior of the rotor wake system. The rotor wake can be described as a cylindrical column of accelerated flow which is skewed from the freestream direction by an angle determined from the downward velocity within the wake and the freestream velocity magnitude. The resulting angle from the vertical for the average wake trajectory is known as the skew angle, X. Using the analysis of Stepniewski and Keys (1984) a derivation of skew angle for a rotor in forward flight can be found as:

$$X = \tan^{-1} (V \cos(\alpha)/(v_f - V \sin(\alpha)))$$

where V is the freestream velocity, α is the rotor shaft angle of attack, and v_f is a function of rotor thrust coefficient and freestream velocity.

For this rotor system, operating at a rotor thrust coefficient of 0.0064 and a rotational speed of 209 rad/s, the following table shows the skew angle calculated from the above reference for a rotor in forward flight. Also included in the table are the skew angles determined from the experimental data found by Ghee *et al* (1996) as well as the skew angle measured in the DGV data and discussed below the table.

Freestream Velocity, V, m/s	9	27.7	42
α, deg	0	-3	-3
v_f, m/s	10.6	3.7	2.5
X, deg - Theoretical	40	79	84
X, deg - Experimental Flow Vis (Ghee, *et al* (1996))	NA	77	79
X, deg - DGV Experimental Images	57	78	83

Figures 13 and 14 show a DGV image of the freestream velocity component for a rotor position of zero degrees azimuth for the 27.7 and 42.0 m/s test conditions, respectively. The view in the image is from the right side of the model looking inboard at the 80-percent radial location. The flow is from right to left in the figures, and the rotor blade is rotating from left to right. The grayscale in the image indicates where the smoke was observed in the field of view. The black areas are the absence of the seeding smoke. In each image, the center of the hub is located by a small crosshair and the blades are overlaid at their forward and aft positions. The overlaid dot card pattern gives a sense of scale with 6.35 cm spacing between the dots.

The long dashed white line in each of the images highlights the skew angle seen in the DGV measurements. The boundary of the wake should convect downstream at the wake skew angle and should theoretically be along the short dashed lines. However, vortex positions obtained from the flow visualization data (symbols), (Ghee *et al* (1996)), show the location of the wake boundary to match the DGV results for these test conditions. Both theoretical and experimental data indicate good agreement in skew angle.

While the good agreement of skew angle is a positive indication for the DGV measurement, further comparisons with wind tunnel freestream data and with independent, three-component laser velocimetry data have been limited by the thermal variations in the Iodine calibrations and low frequency variations in the scattered light. Calibration corrections based on cell temperature measurements obtained for every image are underway at this time to improve the DGV data for later comparisons. Also, laboratory investigations are underway to determine the source of the low frequency variations in the normalized signal image not found in the Argon-ion laser based system.

Rotor Blade Deformation Measurements

PMI was successfully used to measure the rotor blade deformation. Figure 15 shows the contours of the blade deformation for several test conditions, and differences in the blade shape are clearly visible. The blade shape deforms as would be expected for a rotor system undergoing changes in test condition; the most dramatic tip deformation relative to the horizontal reference plane occurred when the rotor shaft angle was tilted forward. Figure 16 shows the change in measured blade height with rotor azimuth for the rotor tip path plane tilted 3 degrees nose down. The measured 26 mm difference in the blade tip deflection between 70 and 110 degrees of azimuth corresponds well to the expected deflection due to the geometry of 32 mm.

Lessons Learned

Three-component flow field investigations using DGV to conditionally sample an unsteady flow field in a large wind tunnel facility illustrates the vast differences between laboratory and large wind tunnel environments. The tasks where difficulties were anticipated such as combining the DGV and PMI systems, synchronizing the lasers, cameras, and data acquisition computers, and conditionally sampling the measurements as a function of rotor azimuth, were very successful. Several areas have been identified where previous experience was insufficient to predict system characteristics. These included insufficient isolation of the Iodine vapor cells from the tunnel environment, laser speckle, and other noise sources originating from the Nd:YAG laser.

From these experiences, the following modifications to the system and procedures are recommended:

1. Procedures must be developed to prevent laser damage to wind tunnel models.

2. Vapor pressure limited Iodine vapor cells completely isolated from the wind tunnel environment need to be developed.

3. Vibration isolate the Nd:YAG laser and place it totally out of the flow field.

4. Develop a smoke generating system that will yield smoke plumes at least 1.5 m in diameter, preferably using cold injection.

5. Use the rotor synchronized Argon-ion based laser light sheet system to set the smoke plume position.

Summary

The first attempt to use pulsed, three-component Doppler Global Velocimetry to measure unsteady rotor wake flow fields was presented. These conditionally sampled results were accompanied by the simultaneously acquired pulsed laser Projection Moiré Interferometry deformation and twist measurements of the moving rotor blades. While the PMI results were very successful, the DGV results suffered from environmental problems and image noise originating by the Nd:YAG laser. The vapor-limited Iodine cell was found to be less sensitive to the environmental changes than the standard cells. Median filtering techniques virtually eliminated laser speckle noise while preserving

details of the vortex structures. Work continues on reducing noise sources and correcting the data for temperature induced calibration changes.

References

Astola, J. and Kuosmanen, P.: **Fundamentals of Nonlinear Digital Filtering**. CRC Press, New York, 1997.

Elliott, J. W.; Althoff, S. L.; and, Sailey, R. H.: *Inflow Measurement Made With a Laser Velocimeter on a Helicopter Model in Forward Flight*. Volumes I-III, NASA TM 100541-100543, AVSCOM TM 88-B-004-006, April, 1988.

Fleming, G. A. and Gorton, S. A.: *Measurement of Rotorcraft Blade Deformation using Projection Moiré Interferometry*. Proceedings of the 3rd International Conference on Vibration Measurements by Laser Techniques, Ancona, Italy, June 16-19, 1998.

Gentry, G. L., Jr.; Quinto, P. F.; Gatlin, G. M.; and, Applin, Z. T.: *The Langley 14-by 22-Foot Subsonic Tunnel — Description, Flow Characteristics, and Guide for Users*. NASA TP-3008, 1990.

Ghee, T. A.; Berry, J. D.; Zori, L. A. J.; and, Elliott, J. W.: *Wake Geometry Measurements and Analytical Calculations on a Small-Scale Rotor Model*. NASA TP 3584, ATCOM TR-96-A-007, August 1996.

Komine, H.: *System for Measuring Velocity Field of Fluid Flow Utilizing a Laser -Doppler Spectral Image Converter*, US Patent 4 919 536, 1990.

Komine, H.; Brosnan, S. J.; Long, W. H.; and Stappaerts, E. A.: *Doppler Global Velocimetry Development of a Flight Research Instrumentation System for Application to Non-intrusive Measurements of the Flow Field*, NASA Report CR-191490, 1994.

McKenzie, R. L.: *Planar Doppler Velocimetry for Large-Scale Wind Tunnel Applications*. AGARD Fluid Dynamics Panel 81st Meeting and Symposium on Advanced Aerodynamic Measurement Technology, paper 9, Seattle, WA, September 22-25, 1997.

Meyers, J. F.: *Doppler Global Velocimetry - The Next Generation?* AIAA 17th Aerospace Ground Testing Conference, paper AIAA-92-3897, Nashville, TN, July 6-8, 1992.

Meyers, J. F.: *Development of Doppler Global Velocimetry as a Flow Diagnostics Tool*, Measurement in Fluids and Combustion Systems, Special Issue, Measurement Science and Technology, vol 6, no. 6, pp. 769-783, June 1995.

Meyers, J. F.: *Evolution of Doppler Global Velocimetry Data Processing*. Eighth International Symposium on Applications of Laser Techniques to Fluid Mechanics, paper 11.1, Lisbon, Portugal, July 8-11, 1996.

Smith, M. W.: *Application of a Planar Doppler Velocimetry System to a High Reynolds Number Compressible Jet*. AIAA 36th Aerospace Sciences Meeting & Exhibit, paper AIAA 98-0428, Reno, NV, January 12-15, 1998.

Stepniewski, W. Z.; and, Keys, C. N.: **Rotary-Wing Aerodynamics**. Dover Publications, Inc., New York, 1984

Figure 1.-The Langley 14-by 22-Foot Subsonic Tunnel.

Figure 2.-The 1.7-meter isolated rotor system with the fuselage placed below the rotor mounted in the 14-by 22-Foot Subsonic Tunnel.

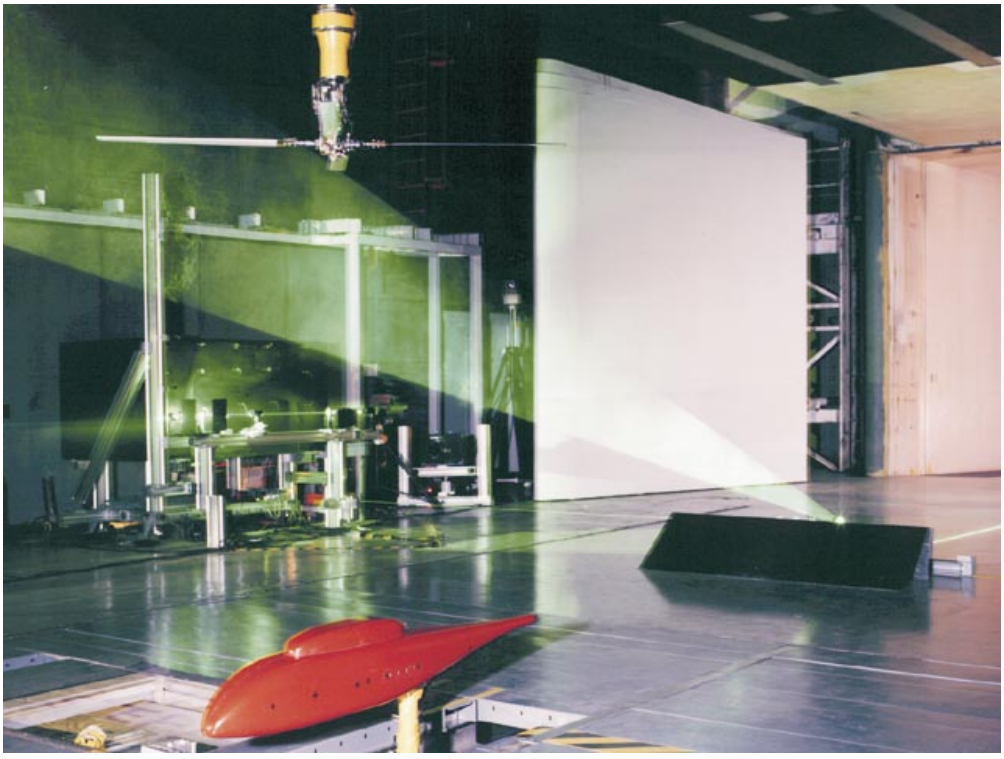

Figure 3.-The 1.7-meter isolated rotor system with the fuselage placed out of the flow.

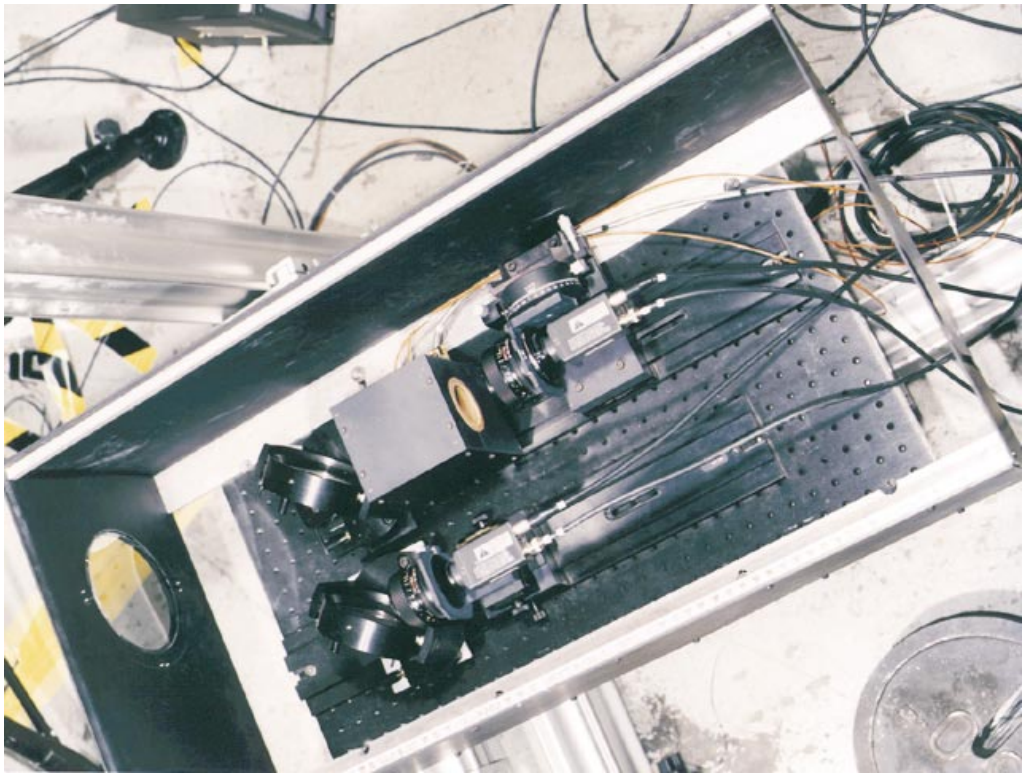

Figure 4.-Doppler Global Velocimeter receiver optical system.

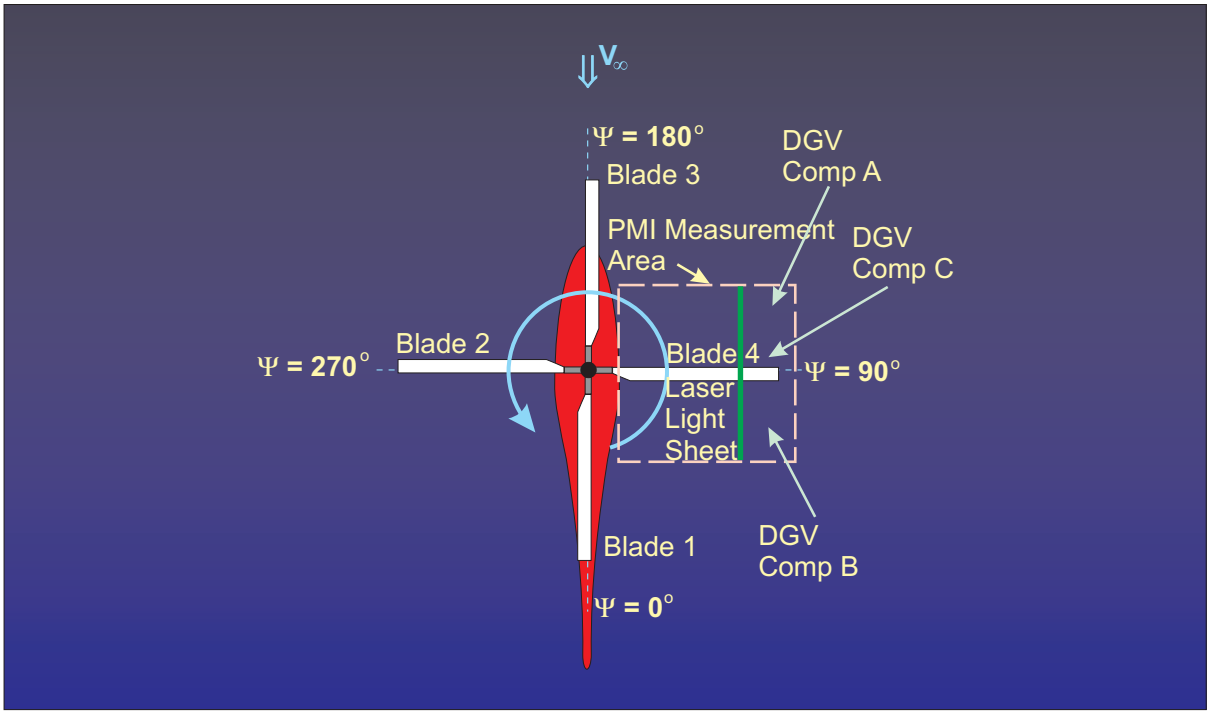

Figure 5.-Planview of the model, laser light sheet, DGV receiver optical systems, and PMI measurement area.

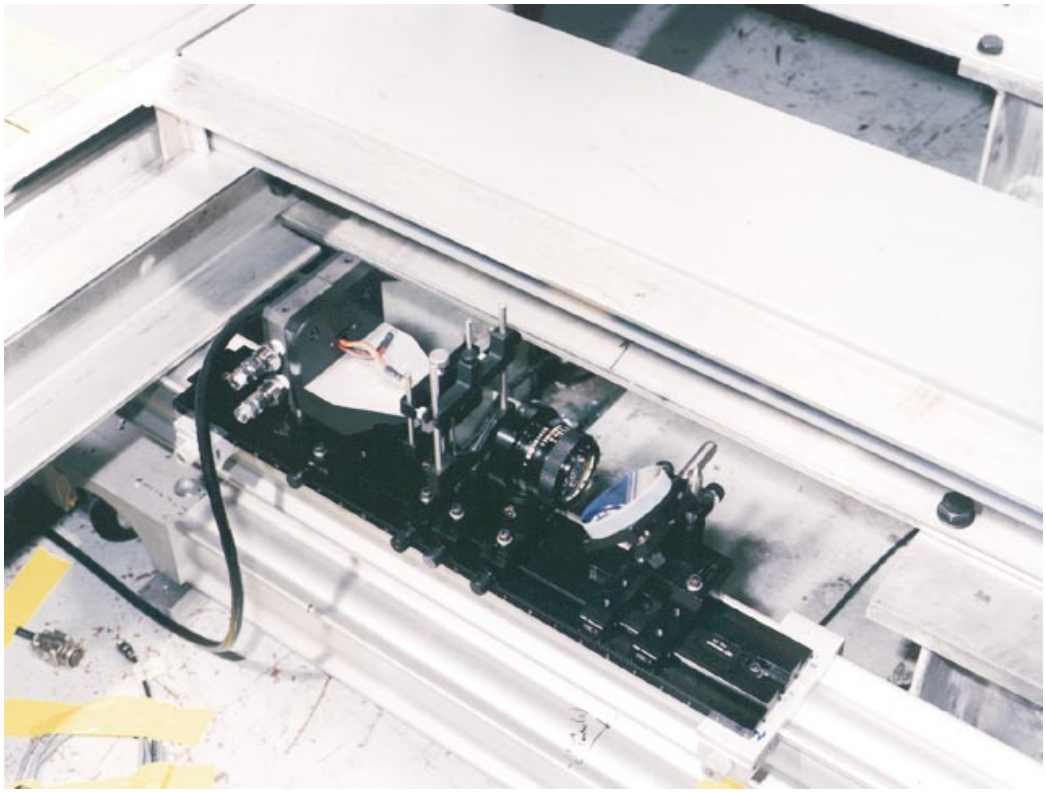

Figure 6.-Projection Moiré Interferometer laser and transmission optical system.

Figure 7.-Alignment and spatial calibration target for DGV and PMI.

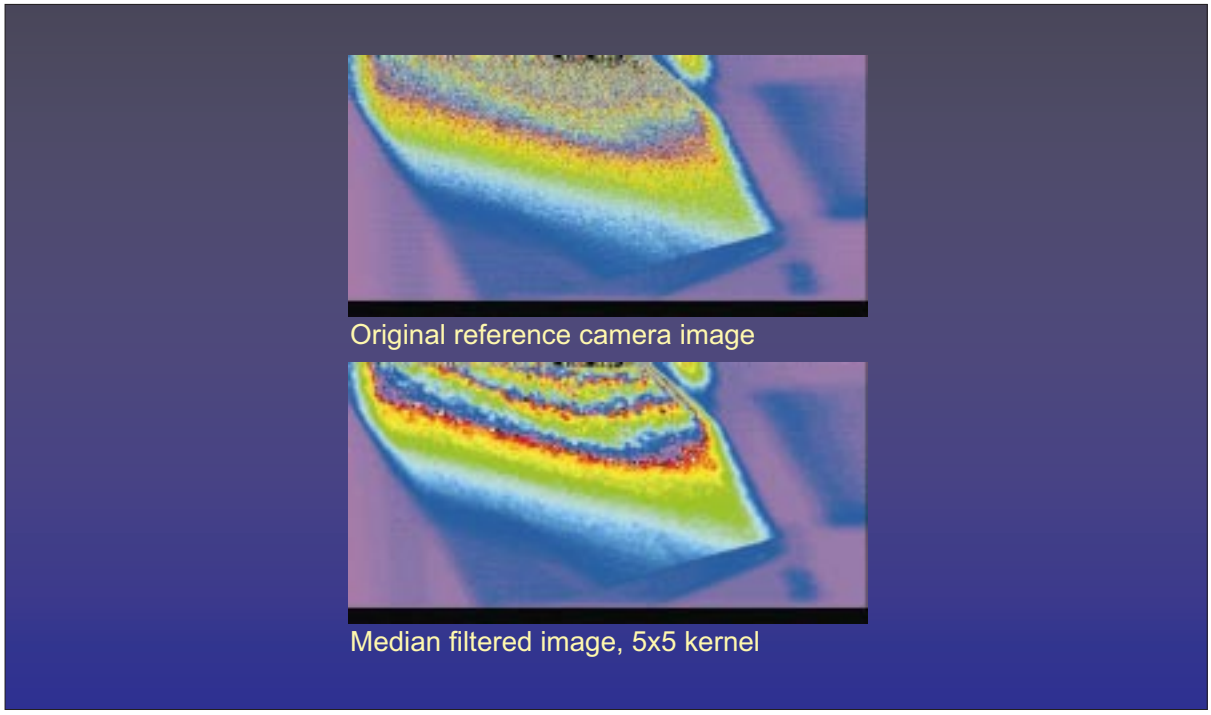

Figure 8.-Removal of laser speckle noise with a median filter.

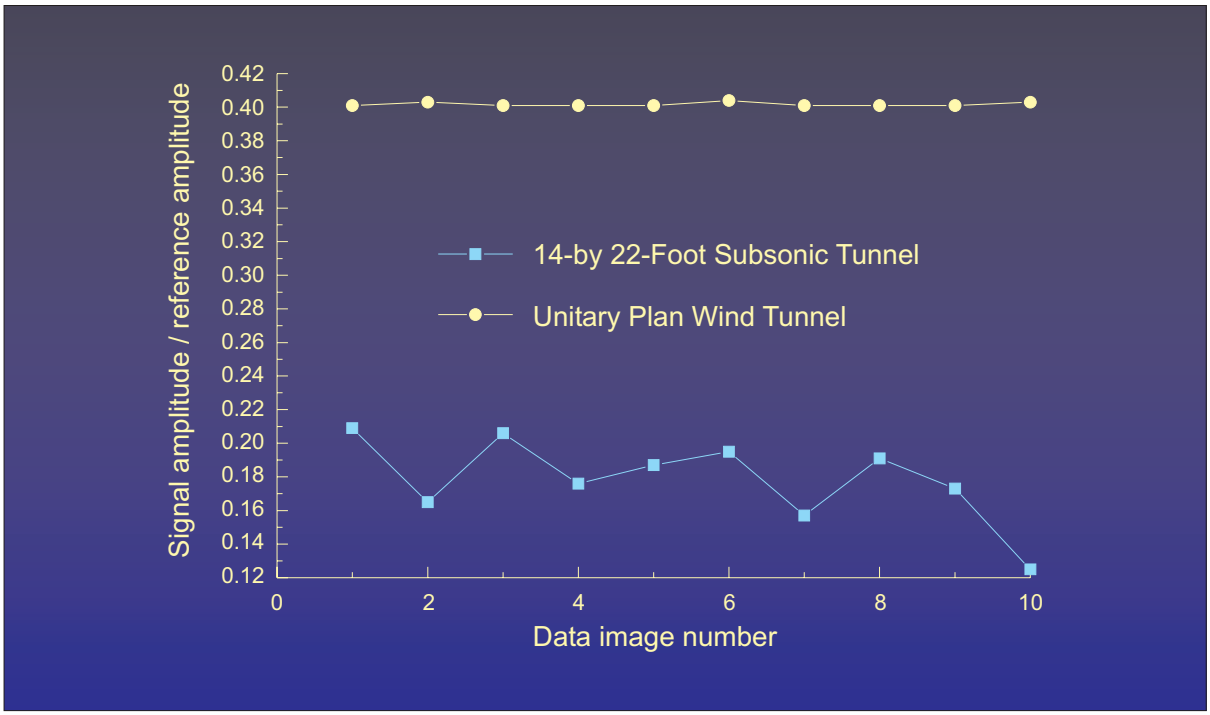

Figure 9.-Comparison of Nd:YAG laser frequency stability during two wind tunnel tests.

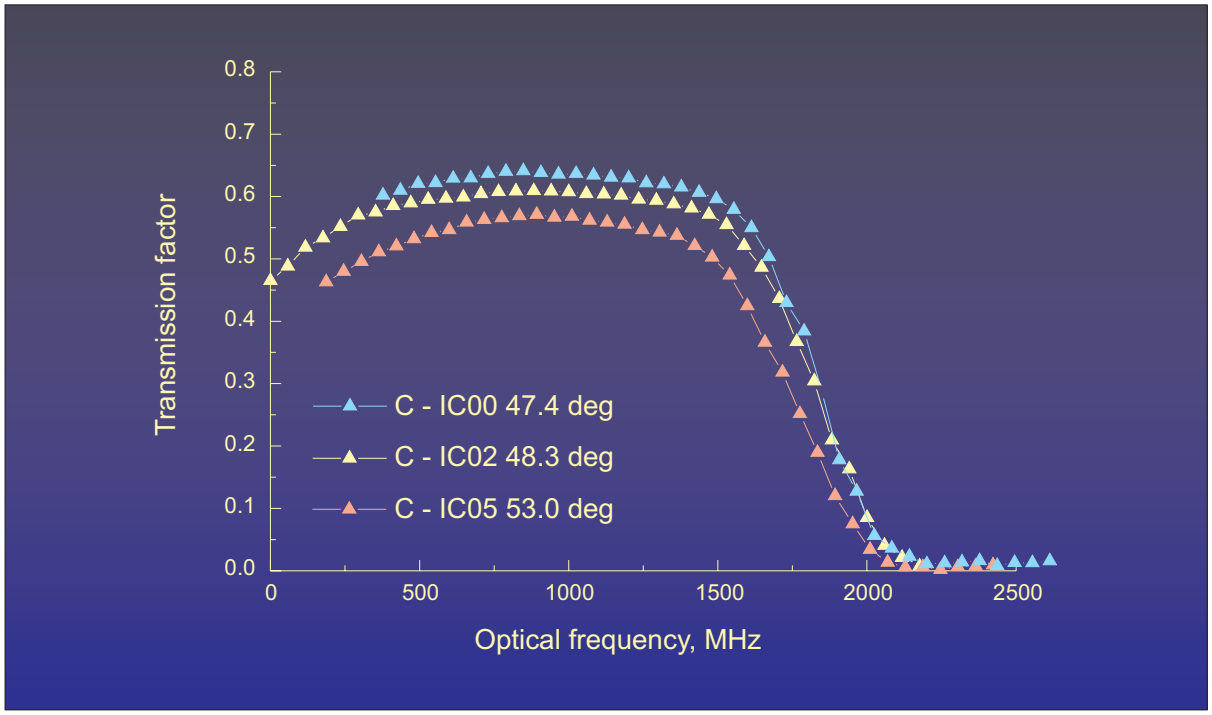

Figure 10.-Iodine vapor cell calibrations for component C before, during, and after a typical tunnel run.

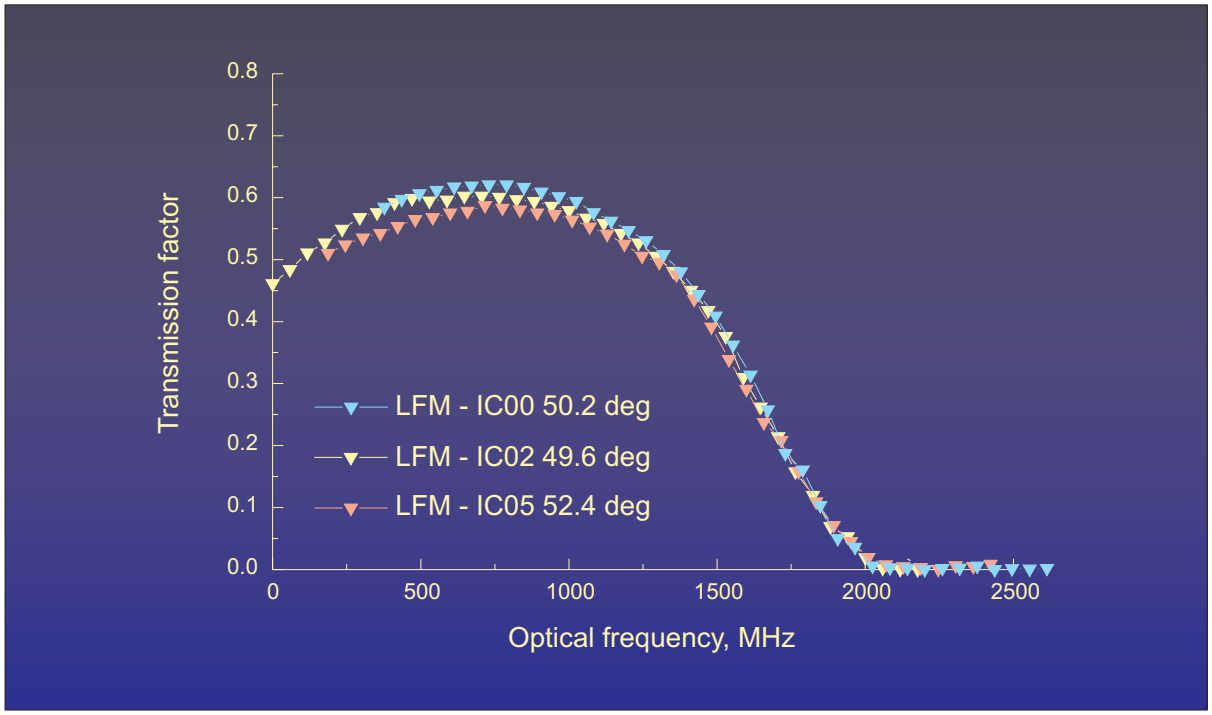

Figure 11.-Iodine vapor cell calibrations for the laser frequency monitor obtained simultaneously with Figure 10.

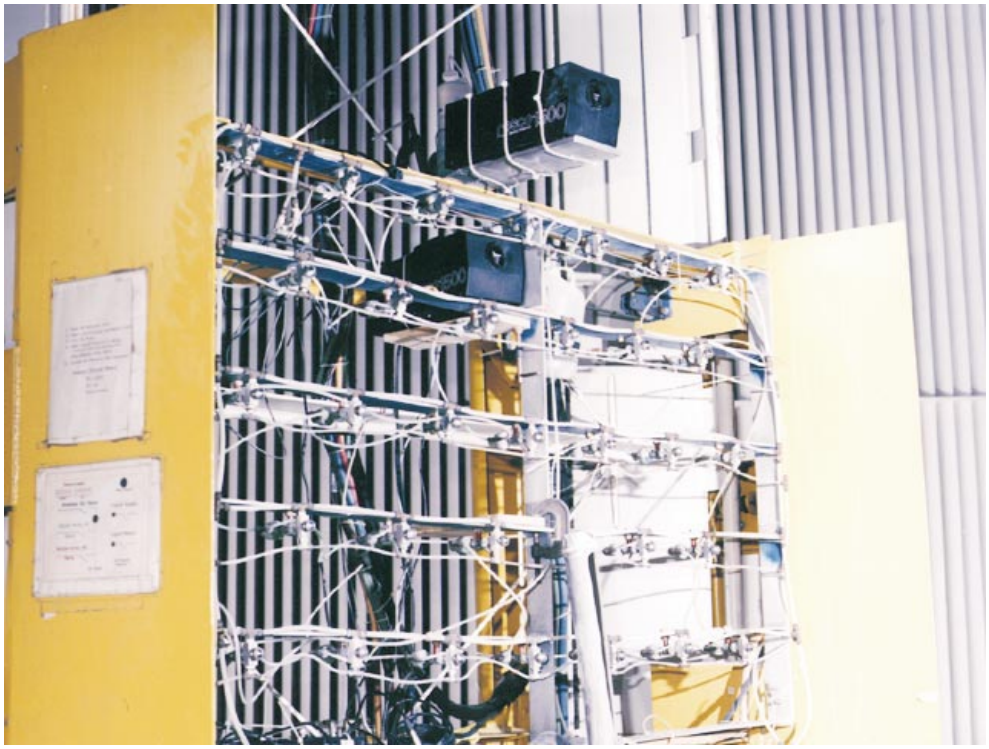

Figure 12.-Vaporization/condensation smoke generators attached to the laser velocimeter particle generation nozzle array in the tunnel settling chamber.

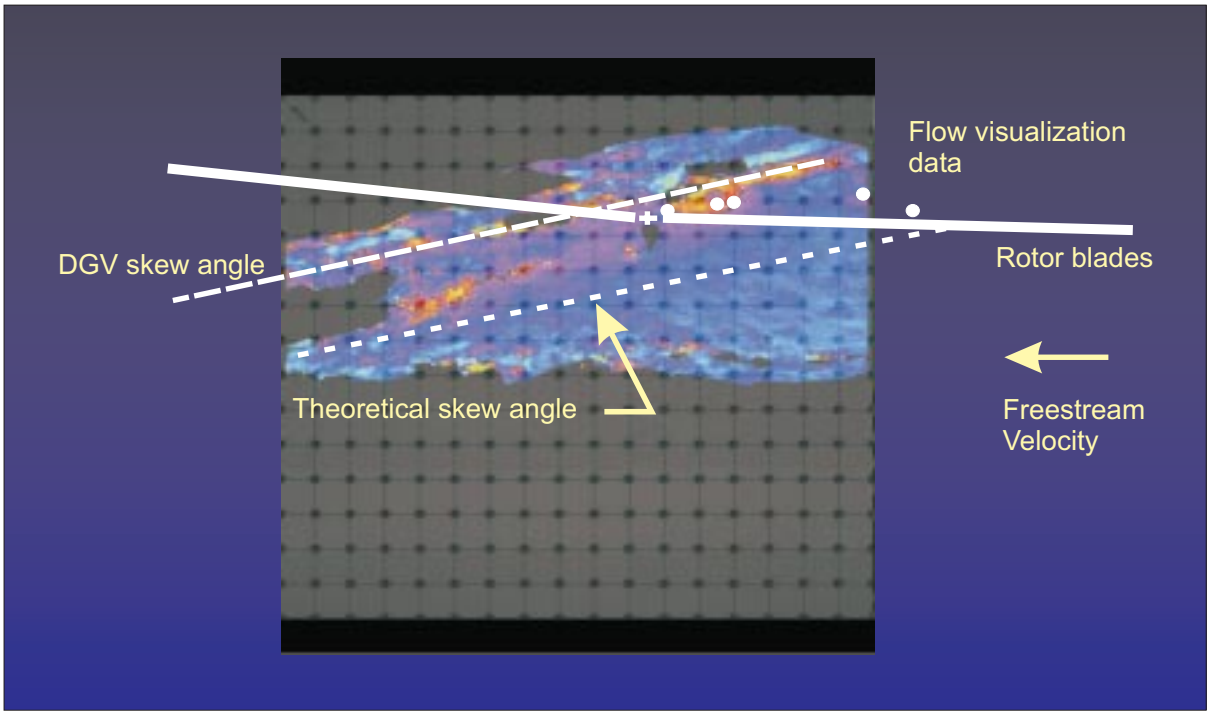

Figure 13.-DGV measurement of the streamwise velocity with overlays of theoretical rotor wake skew angle and vortex positions obtained from flow visualization, freestream velocity = 27.7 m/s.

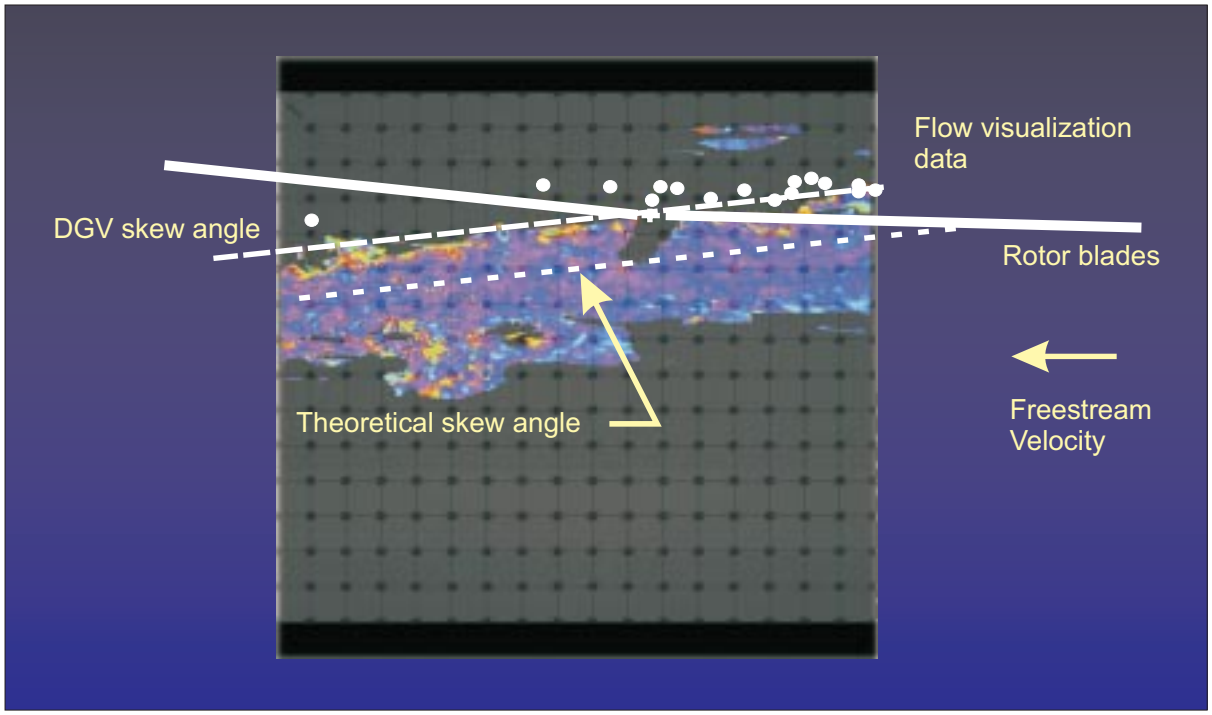

Figure 14.-DGV measurement of the streamwise velocity with overlays of theoretical rotor wake skew angle and vortex positions obtained from flow visualization, freestream velocity = 42.0 m/s.

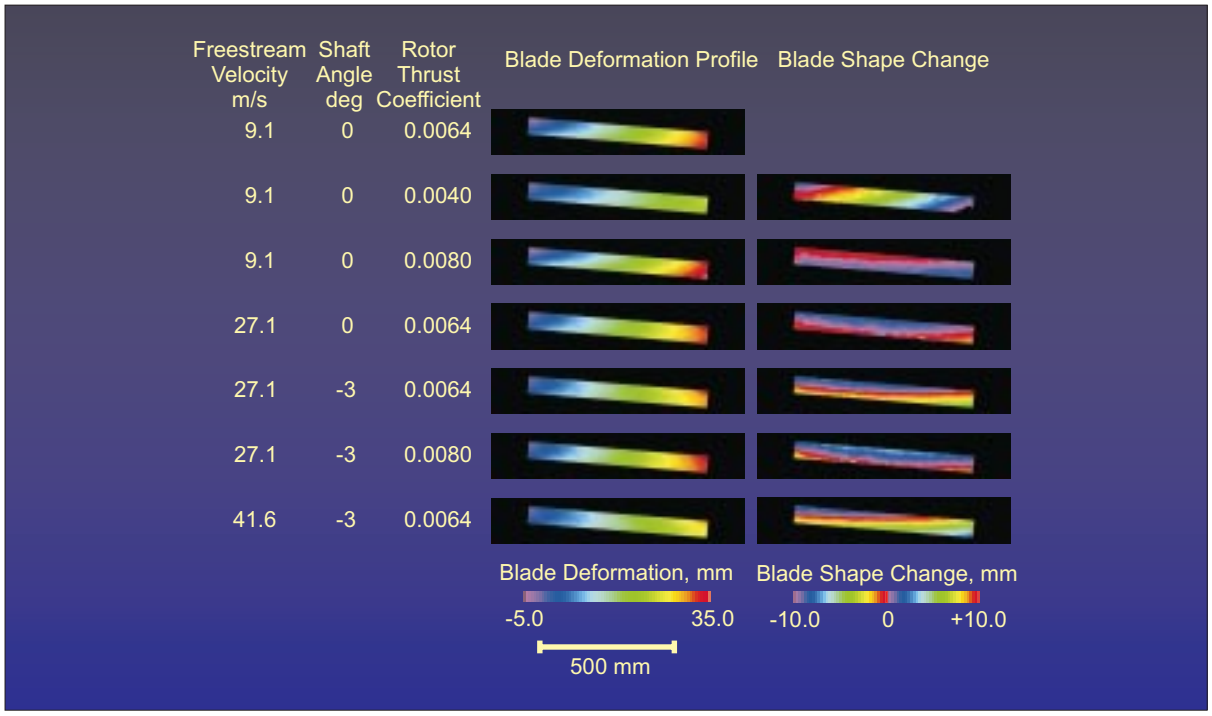

Figure 15.-PMI measured blade deflection profiles for seven different flight conditions, blade #4.

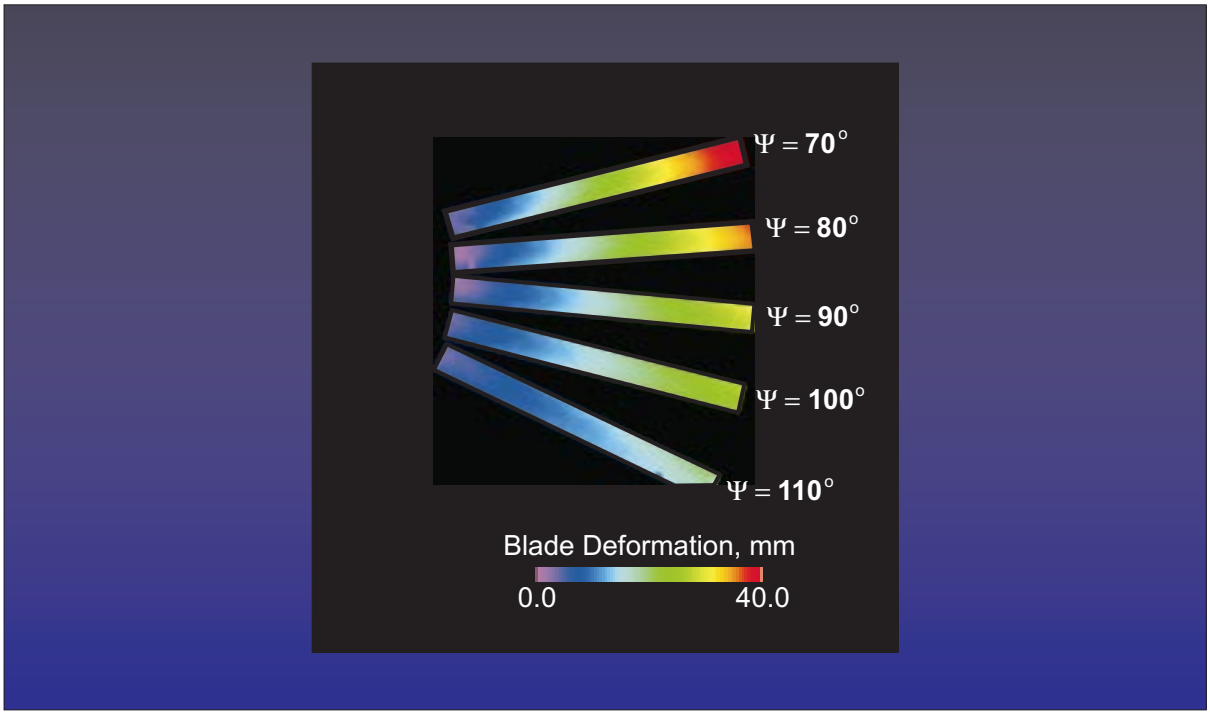

Figure 16.-Azimuth dependent PMI measured blade deformation profiles, fuselage down, rotor shaft angle set to -3 degrees.